

# A Metal-Based Lumophore Tailored To Sense Biologically Relevant Oxometalates\*\*

Anna F. A. Peacock, Helen D. Batey, Claudia Raendler, Adrian C. Whitwood, Robin N. Perutz,\* and Anne-K. Duhme-Klair\*

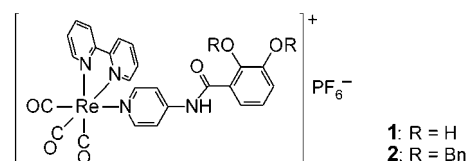
Catechol–lumophore conjugates are attracting increasing interest as supramolecular photochemical devices, with potential applications as sensors,<sup>[1]</sup> redox switches,<sup>[2]</sup> and photo- and electrocatalysts.<sup>[3]</sup> The versatility of the conjugates results from the redox activity of the catechol moiety, the oxidation potential of which can be modulated by pH control and metal ion coordination.<sup>[4]</sup> Once deprotonated, the negatively charged catecholate oxygen donors are well suited to chelate chemically hard metal ions in high oxidation states.<sup>[5]</sup>

As metal ions in high oxidation states typically form oxometalate anions in aqueous media, a selective analytical technique must be directed at anions. There is interest in the analysis of oxometalate ions, such as molybdate, for several types of application. Environmental monitoring of molybdate is required as excessive soil molybdate causes molybdenosis in ruminants;<sup>[6]</sup> biochemical monitoring is needed to understand molybdate uptake<sup>[7]</sup> and the recently discovered link between  $\text{MoO}_4^{2-}$  and  $\text{Cu}^{2+}$  metabolism.<sup>[8]</sup> Medical analysis is of interest as deficiency of Mo cofactor causes neurological disorders.<sup>[9]</sup> A sensor that is selective for oxometalates must not only compete successfully with other oxoanions, such as  $\text{SO}_4^{2-}$  and  $\text{HPO}_4^{2-}$ , but also with metal cations, such as  $\text{Fe}^{3+}$  and  $\text{Cu}^{2+}$ .

Although the development of luminescent sensors and probes for anions is an emerging field,<sup>[10]</sup> as yet, no selective chemosensors for biologically important oxometalates are available on the market,<sup>[11]</sup> and studies that target these oxometalates are rare.<sup>[12]</sup> Promising approaches to molybdate sensing include catalytic fluorometric methods<sup>[12b]</sup> and the quenching of the fluorescence of organic ligands by  $\text{Mo}^{\text{VI}}$ .<sup>[12a,c]</sup> Furthermore, heteroditopic ion-pair receptors were recently designed for the sequestration of environmentally deleterious oxometalates, such as  $\text{ReO}_4^-$  and  $\text{TcO}_4^-$ , which were bound as  $\text{Na}^+$  salts through a combination of hydrogen-bonding and electrostatic interactions.<sup>[13]</sup>

In pursuit of an optical detection method for early-transition-metal ions in high oxidation states, we have recently taken a supramolecular two-component approach in the development of a catechol– $[\text{Ru}^{\text{II}}(2,2'\text{-bpy})_3]^{2+}$  (bpy = bipyridine) conjugate, which signals the presence and concentration of molybdate ( $\text{MoO}_4^{2-}$ ) in solution through luminescence quenching.<sup>[1c,d]</sup> In this prototype sensor, the metal-binding catechol unit is separated from the lumophore by an alkyl chain. In principle, the long excitation and emission wavelengths and large Stokes shifts of metal-based lumophores, such as Ru- and Re-polypyridyl complexes, are advantageous for measurements in biological media, provided that the compatibility of the complexes with water is improved.

Here we report the design, synthesis, and luminescent properties of a second-generation sensor **1** based on a



$[\text{Re}^{\text{I}}(2,2'\text{-bpy})(\text{py})(\text{CO})_3]^+$  chromophore (py = pyridine). In **1**, the catechol unit is linked directly to the monodentate pyridyl ligand of the chromophore. The electron-withdrawing effect of the  $\pi$ -deficient pyridyl group which is enhanced by the coordinated positively charged chromophore increases the acidity of the phenolic OH groups. This has two main advantages: First, the affinity of the sensor for Mo at low pH values is increased, and second, the system is stabilized against air oxidation. Furthermore, the amide linker facilitates electron transfer from the catecholate quencher to the photoexcited chromophore as it ensures the planarity of the ligand. The  $[\text{Re}^{\text{I}}(\text{bpy})(\text{py})(\text{CO})_3]^+$  chromophore was selected for the ease with which it is derivatized, its long-lived luminescence, and its photochemical stability.<sup>[14]</sup>

The benzyl (Bn)-protected pyridine ligand  $\text{Bn}_2\text{L}$  (2,3-dibenzyloxybenzoyl-4-aminopyridine) was synthesized by condensation of 2,3-dibenzyloxybenzoic acid chloride<sup>[15]</sup> with 4-aminopyridine by an analogous procedure to that reported by MacQueen and Schanze.<sup>[14a]</sup>  $\text{Bn}_2\text{L}$  was then heated at reflux with rhenium tricarbonyl bipyridyl bromide and silver triflate in THF to form the benzyl-protected complex, which was isolated as the  $\text{PF}_6^-$  salt **2**, upon addition of  $\text{NH}_4\text{PF}_6$ , in 60% yield. Complex **2** was characterized by ES mass spectrometry, IR and NMR spectroscopy, as well as X-ray crystallography (Figure 1).<sup>[16]</sup> The coordination geometry of the rhenium center in **2** is distorted octahedral and typical for bipyridine-coordinated *fac*- $\text{Re}^{\text{I}}(\text{CO})_3$  units.<sup>[17]</sup> The crystal structure confirms that the core of **L** is held essentially planar by an intramolecular hydrogen bond between the amide proton and the adjacent 2-benzyloxy donor (distance  $\text{N}(4)\cdots\text{O}(5) = 2.64(1) \text{ \AA}$ ). The dihedral angle between the catechol moiety and the pyridine ring deviates by  $7.6(2)^\circ$  from an ideal coplanar orientation.

Complex **2** was debenzylated by catalytic hydrogenolysis to give **1** and the product was identified by TLC, mass spectrometry, and NMR spectroscopy. The solubility of **1**, and

[\*] A. F. A. Peacock, H. D. Batey, C. Raendler, Dr. A. C. Whitwood, Prof. R. N. Perutz, Dr. A.-K. Duhme-Klair  
Department of Chemistry  
University of York  
York YO10 5DD (United Kingdom)  
Fax: (+44) 190-443-2516  
E-mail: akd1@york.ac.uk

[\*\*] We thank the EPSRC and the EU for financial support and Dr. Nicole Reddig for experimental assistance.

Supporting information for this article is available on the WWW under <http://www.angewandte.org> or from the author.

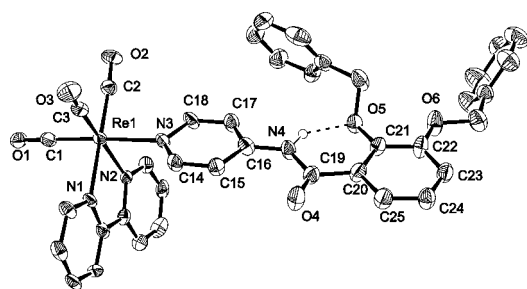


**Figure 1.** ORTEP plot of  $[\text{Re}(\text{2,2'}\text{-bpy})(\text{Br}_2\text{L})(\text{CO})_3]^+$  (50% probability ellipsoids). Hydrogen atoms, except that at the amine (N4), are omitted for clarity. Selected bond lengths [Å]: Re–C1 1.917(8), Re–C2 1.921(8), Re–C3 1.926(8), Re–N1 2.168(5), Re–N2 2.160(6), Re–N3 2.219(6).

in particular **2**, in water is limited. To allow a comparison of the spectroscopic properties of **1** and **2**, the solvent system used throughout the studies consisted of 95:5 acetonitrile/water. In studies with **1**, however, the water content of the solvent mixture can be increased up to 20% without apparent precipitation or loss of sensor activity (see Supporting Information).<sup>[18]</sup> As acetonitrile is miscible with water, it is possible to detect metal ions that are added in aqueous solution. Furthermore, the pH range for the detection can be established and adjusted by using standard buffer solutions.

Excitation at 370 nm into the  $\text{Re}(\text{d}\pi) \rightarrow \text{bpy}(\pi^*)$  charge-transfer bands<sup>[14,17]</sup> of **1** and **2** gives rise to broad emission bands around 565 nm. Whereas the emission spectrum of **2** is pH-independent between pH 0.1 and 10, the emission of the “free” sensor **1** shows a sigmoidal decrease in intensity due to the deprotonation of the OH group in the *ortho* position (Figure 2). The pH dependence of luminescence gives an apparent  $\text{p}K_{\text{a}}$  value of around 4.9 for **1**, which is comparatively low for a catecholamide.<sup>[1c,19]</sup> The maximum emission intensity of **1** observed at low pH, however, is still approximately 30% lower than that of **2**.

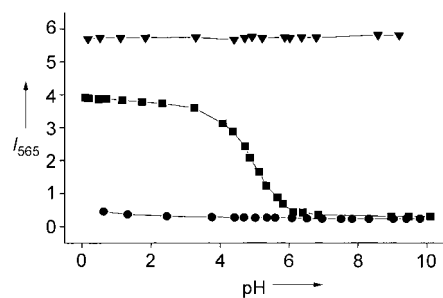


**Figure 2.** Intensity of emission at maximum ( $\lambda_{\text{em}} = 565$  nm) versus pH for **2** (▼), **1** (■), and **1** in the presence of molybdate (0.5 equiv; ●).  $\lambda_{\text{ex}} = 370$  nm, solutions in aqueous acetonitrile.

The addition of 0.5 equivalents of molybdate<sup>[20]</sup> results in quenching of the emission, indicating strong binding of the analyte. To gain further insight into the stoichiometry of the molybdenum complex formed, a solution of **1**, buffered at pH 4, was titrated with molybdate (Figure 3). Upon addition of molybdate, the emission intensity decreased gradually.

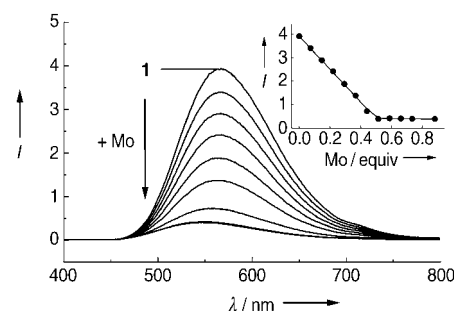
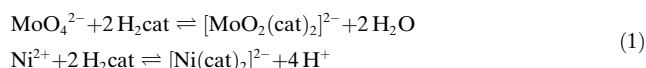


**Figure 3.** Emission spectra (uncorrected) of **1** ( $10^{-4}$  M) in the presence of increasing concentrations of molybdate (in aqueous acetonitrile at pH 4.0, buffer: 2,6-lutidine,  $\lambda_{\text{ex}} = 370$  nm). Inset: Emission intensity at 565 nm as a function of molar equivalents of  $\text{MoO}_4^{2-}$ .

Apart from a slight shift of the emission maximum toward shorter wavelengths at high levels of molybdate, no other spectral changes were observed. The emission intensity decreases linearly up to a clear break at a ratio of Mo/**1** of 0.5, consistent with the formation of a 1:2 molybdenum/catecholate complex. The response fits<sup>[21]</sup> to an apparent overall binding constant of  $\log \beta'_2 = 13(\pm 1)$ . Under these conditions, the detection limit was determined to be  $55 \mu\text{g L}^{-1}$ .<sup>[18]</sup>

Next, the selectivity of **1** was investigated by repeating the titration of the solution of the acidic sensor with standard base in the presence of potentially interfering ions. The pH profiles obtained in the presence of metal cations, such as  $\text{Co}^{2+}$ ,  $\text{Ni}^{2+}$ ,  $\text{Cu}^{2+}$ ,  $\text{Zn}^{2+}$ , and  $\text{Fe}^{3+}$ , do not differ significantly from that obtained for the titration of **1** alone (see Supporting Information). The lack of quenching in the low pH region may be rationalized by the stronger pH dependence of the reaction of metal cations with catechols [Eq. (1), cat = catechol]. The pH profiles obtained in the presence of oxoanions, such as sulfate or phosphate, are almost identical to the pH profile of **1** (see Supporting Information). This absence of interference is particularly advantageous for biological applications, where high concentrations of sulfate and phosphate ions are likely to be present.



In the presence of tungstate,<sup>[20]</sup> the initial emission intensity at low pH values decreases slightly, probably owing to the heavy-atom effect; the  $\text{p}K_{\text{a}}$  value, however, is not shifted significantly (Figure 4). As the coordination chemistry of Mo is very similar to that of W, the unexpectedly high selectivity for molybdate over tungstate under acidic conditions merited further investigations. We therefore examined the reversibility of the titrations in detail. Whereas the response of **1** in the absence and in the presence of most of the ions tested was independent of the direction of the titration (low to high pH, or high to low pH), the pH profile obtained in the presence of tungstate revealed hysteresis-type behavior. The lack of quenching during the forward titration (low to high pH) may be related to the formation of polyoxometalates. Both W and Mo form polyoxometalates

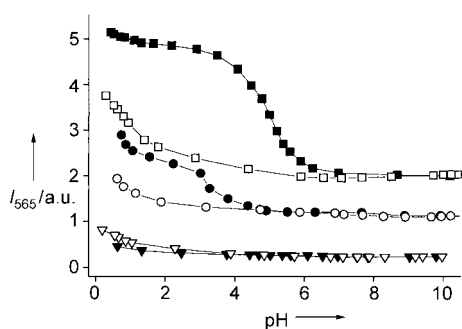


**Figure 4.** Reversibility studies with solutions containing **1** in the presence of the following oxometalates (0.5 equiv): tungstate (■, □), vanadate (●, ○), and molybdate (▼, ▽). Titrations from low to high pH: solid symbols; from high to low pH: hollow symbols. Offset: 0.8 a.u. each.

in acidic solutions; however, the Mo-containing species react quickly, whereas the W-containing species are known to be more inert.<sup>[22]</sup> This allows kinetic differentiation of the two analytes.

As molybdenum is diagonally related to vanadium as well as rhenium, vanadate and perrhenate ions were also tested. Whereas perrhenate gave no response (see Supporting Information), vanadate<sup>[20]</sup> was found to be the only other biologically relevant ion investigated that also quenches the emission of **1**. During the forward titration, the emission intensity of **1** decreases significantly in the low pH region, indicating a moderate binding affinity toward vanadate. The pH profile obtained is more complicated in shape, and the back titration reveals hysteresis-type behavior. Further studies are required to identify the vanadium-containing species that are involved in the underlying equilibria.

In conclusion, we have developed a new selective high-affinity chemosensor for the most biologically relevant oxometalates: molybdate, tungstate, and vanadate. The sensor system operates in up to 20% (v/v) H<sub>2</sub>O in CH<sub>3</sub>CN in the pH range 0.1–4.5 and indicates binding of the analyte by efficient quenching of the (Re–bipyridyl)-based luminescence.

Received: October 14, 2004

Published online: February 3, 2005

**Keywords:** luminescence · molybdenum · oxo ligands · sensors

- [1] a) P. D. Beer, *Chem. Commun.* **1996**, 689; b) I. Costa, L. Fabbrizzi, P. Pallavicini, A. Poggi, A. Zani, *Inorg. Chim. Acta* **1998**, 275–276, 117; c) S. B. Jedner, R. J. James, R. N. Perutz, A.-K. Duhme-Klair, *J. Chem. Soc. Dalton Trans.* **2001**, 2327; d) S. B. Jedner, R. N. Perutz, A.-K. Duhme-Klair, *Z. Anorg. Allg. Chem.* **2003**, 629, 2421; e) L. O'Brien, M. Duati, S. Rau, A. L. Guckian, T. E. Keyes, N. M. O'Boyle, A. Serr, H. Görls, J. G. Vos, *Dalton Trans.* **2004**, 514.
- [2] V. Goulle, A. Harriman, J.-M. Lehn, *J. Chem. Soc. Chem. Commun.* **1993**, 1034.
- [3] a) B. Whittle, N. S. Everest, C. Howard, M. D. Ward, *Inorg. Chem.* **1995**, 34, 2025; b) A. D. Shukla, B. Whittle, H. C. Bajaj, A. Das, M. D. Ward, *Inorg. Chim. Acta* **1999**, 285, 89; c) G. D. Storrier, K. Takada, H. D. Abruna, *Inorg. Chem.* **1999**, 38, 559.

- [4] D. E. Wheeler, J. H. Rodriguez, J. K. McCusker, *J. Phys. Chem. A* **1999**, 103, 4101.
- [5] a) C. G. Pierpont, R. M. Buchanan, *Coord. Chem. Rev.* **1981**, 38, 45; b) C. G. Pierpont, C. W. Lange, *Prog. Inorg. Chem.* **1994**, 41, 331.
- [6] J. Mason, *Toxicology* **1986**, 42, 99.
- [7] R. N. Pau, D. M. Lawson in *Metal Ions in Biological Systems* (Eds.: H. Sigel, A. Sigel), Marcel Dekker, New York, **2002**, 32.
- [8] J. Kuper, A. Llamas, H.-J. Hecht, R. R. Mendel, G. Schwarz, *Nature* **2004**, 430, 803.
- [9] a) V. E. Shih, I. F. Abrams, J. L. Johnson, M. Carney, R. Mandell, R. M. Robb, J. P. Cloherty, K. V. Rajagopalan, *N. Engl. J. Med.* **1977**, 297, 1022; b) C. Kisker, H. Schindelin, A. Pacheco, W. A. Wehbi, R. M. Garrett, K. V. Rajagopalan, J. H. Enemark, D. C. Rees, *Cell* **1997**, 91, 973.
- [10] P. D. Beer, P. A. Gale, *Angew. Chem.* **2001**, 113, 503; *Angew. Chem. Int. Ed.* **2001**, 40, 486.
- [11] R. P. Haugland, *Handbook of Fluorescent Probes and Research Products*, Molecular Probes, <http://www.probes.com>, **2004**.
- [12] a) B. K. Pal, K. A. Singh, K. Dutta, *Talanta* **1992**, 39, 971; b) S. Kawakubo, H. Suzuki, M. Iwatsuki, *Anal. Sci.* **1996**, 12, 767; c) C. Jiang, J. Wang, F. He, *Anal. Chim. Acta* **2001**, 439, 307, and references therein.
- [13] P. D. Beer, P. K. Hopkins, J. D. McKinney, *Chem. Commun.* **1999**, 1253.
- [14] a) D. B. MacQueen, K. S. Schanze, *J. Am. Chem. Soc.* **1991**, 113, 6108; b) K. S. Schanze, D. B. MacQueen, T. A. Perkins, L. A. Cabana, *Coord. Chem. Rev.* **1993**, 122, 63.
- [15] W. H. Rastetter, T. J. Erickson, M. C. Venuti, *J. Org. Chem.* **1981**, 46, 3579.
- [16] X-ray crystallography: Diffraction data were collected on a Bruker Smart Apex diffractometer using a SMART CCD camera. Structures were solved by direct methods using SHELXS-97 and refined by full-matrix least squares using SHELXL-97 (G. M. Sheldrick, University of Göttingen, Germany, **1997**). All non-hydrogen atoms were refined anisotropically. Hydrogen atoms were placed using a "riding model" and included in the refinement at calculated positions. Crystal data: C<sub>40.5</sub>H<sub>30</sub>F<sub>6</sub>N<sub>4</sub>O<sub>6.5</sub>PRe, *M* = 1007.85, yellow crystals, size 0.13 × 0.08 × 0.03 mm<sup>3</sup>, monoclinic, *P*2<sub>1</sub>/c, *a* = 19.8498(11), *b* = 9.4358(6), *c* = 21.1502(12) Å, β = 95.111(1)°, *U* = 3945.7(4) Å<sup>3</sup>, *Z* = 4, ρ<sub>calcd</sub> = 1.697 g cm<sup>-3</sup>, θ<sub>max</sub> = 25°, MoKα radiation, λ = 0.71073 Å, φ- and ω-scans, *T* = 115 K, 21 632 reflections collected, 6970 independent (*R*<sub>int</sub> 0.0654). Absorption correction was applied using SADABS (v2.03, Sheldrick), μ = 3.203 mm<sup>-1</sup>, 0.797 < *T* < 1.000, multiscan, final *R* = 0.0407 (for *I* ≥ 2σ(*I*)), *wR*(*F*<sup>2</sup>) 0.1114 (all data). CCDC 248500 contains the supplementary crystallographic data for this paper. These data can be obtained free of charge from The Cambridge Crystallographic Data Centre via [www.ccdc.cam.ac.uk/data\\_request/cif](http://www.ccdc.cam.ac.uk/data_request/cif).
- [17] a) V. W.-W. Yam, S. H.-F. Chong, C.-C. Ko, K.-K. Cheung, *Organometallics* **2000**, 19, 5092; b) K. K.-W. Lo, D. C.-M. Ng, W.-K. Hui, K.-K. Cheung, *J. Chem. Soc. Dalton Trans.* **2001**, 2634; c) M. Busby, D. J. Liard, M. Motevalli, H. Toms, A. Vlcek, Jr., *Inorg. Chim. Acta* **2004**, 357, 167.
- [18] See Supporting Information for supplementary figures and experimental details.
- [19] K. N. Raymond, G. Mueller, B. F. Matzkanke, *Top. Curr. Chem.* **1984**, 123, 49.
- [20] The oxometalates were added in the form of concentrated aqueous standard solutions of Na<sub>2</sub>MoO<sub>4</sub>·2H<sub>2</sub>O, Na<sub>2</sub>WO<sub>4</sub>·2H<sub>2</sub>O, NH<sub>4</sub>ReO<sub>4</sub>, and NH<sub>4</sub>VO<sub>3</sub>.
- [21] J. Huskens, H. van Bekkum, J. A. Peters, *Comput. Chem.* **1995**, 19, 409.
- [22] K.-H. Tytko, O. Glemser, *Adv. Inorg. Chem. Radiochem.* **1976**, 19, 239; J. J. Cruywagen, *Adv. Inorg. Chem.* **2000**, 49, 127.